



ELSEVIER

Available online at www.sciencedirect.com

SCIENCE @ DIRECT®

PALAEO

Palaeogeography, Palaeoclimatology, Palaeoecology 212 (2004) 119–140

www.elsevier.com/locate/palaeo

Carbonate oxygen isotope paleoaltimetry: evaluating the effect of diagenesis on paleoelevation estimates for the Tibetan plateau

Carmala N. Garzione^{a,b,*}, David L. Dettman^{c,d}, Brian K. Horton^e

^a*Department of Earth and Environmental Sciences, University of Rochester, Rochester, NY 14627, USA*

^b*Department of Geological Sciences and Cooperative Institute for Research in Environmental Science, University of Colorado, Campus Box 399, Boulder, CO 80309, USA*

^c*Department of Geosciences, University of Arizona, Tucson, AZ 85721, USA*

^d*Research Center for Coastal Lagoon Environments, Shimane University, Matsue, Japan*

^e*Department of Earth and Space Sciences, University of California, Los Angeles, CA 90095, USA*

Received 26 January 2004; received in revised form 28 May 2004; accepted 28 May 2004

Abstract

Carbonate oxygen isotope paleoaltimetry is based on analysis of the $\delta^{18}\text{O}$ value of carbonate precipitated from surface water. Deciphering the diagenetic history is important for establishing whether particular carbonates are accurate recorders of paleosurface waters, which reflect paleoelevation. This study provides examples from southern, east–central, and northeastern Tibet of approaches aimed at evaluating the diagenetic history of lacustrine micrites and pedogenic carbonates. The most desirable technique for avoiding erroneous interpretations related to diagenetic overprinting is to analyze carbonates that are known to be primary, such as aragonitic shell material. In rocks that do not contain shell material, we have compared lacustrine micrites and pedogenic carbonates to diagenetic carbonate phases to determine the effects of diagenesis on the isotopic composition of primary carbonates. Where the potential effects of diagenesis are subtle or ambiguous, we have evaluated the fidelity of the carbonate record from systematic trends in C and O isotopes that agree with other interpretations of paleoenvironment, such as high frequency covariance in C and O that corresponds with changes in the Mg concentration of carbonates. Using these strategies, we have determined that diagenesis has not affected the isotopic composition of carbonates in the Late Miocene–Pliocene Thakkhola graben in southern Tibet and the Oligocene to Pliocene Linxia basin in northeastern Tibet. In the case of Paleogene basins in east–central Tibet, however, ambiguity in data precludes the determination of diagenetic effects.

© 2004 Elsevier B.V. All rights reserved.

Keywords: Tibetan plateau; Paleoaltimetry; Oxygen isotopes; Carbonate; Diagenesis

* Corresponding author. Department of Earth and Environmental Sciences, University of Rochester, Rochester, NY 14627, USA.
E-mail address: garzione@earth.rochester.edu (C.N. Garzione).

1. Introduction

Understanding the elevation history of mountain belts is fundamental to evaluating models for the timing and mechanisms of uplift. Oxygen isotope paleoaltimetry provides surface elevation information that is crucial to deciphering the topographic evolution of mountain belts. This technique is based on the observed relationship of more negative $\delta^{18}\text{O}$ values of meteoric water ($\delta^{18}\text{O}_w$) with increasing elevation (Siegenthaler and Oeschger, 1980; Drummond et al., 1993a; Garzione et al., 2000a; Rowley et al., 2001; Poage and Chamberlain, 2001). The global mean $\delta^{18}\text{O}_w$ vs. altitude gradient is $\sim -0.26\text{‰}/100\text{ m}$; however, this isotopic lapse rate varies locally between $-0.1\text{‰}/100\text{ m}$ and $-0.5\text{‰}/100\text{ m}$ (Poage and Chamberlain, 2001). By sampling surface water or rainfall across a topographic gradient, a local $\delta^{18}\text{O}_w$ vs. altitude gradient can be determined (e.g., Garzione et al., 2000b; Gonfiantini et al., 2001). Oxygen isotope ratios of lacustrine, fluvial, and paleosol carbonates can be used as a gauge of paleoelevation because they are strongly influenced by the $\delta^{18}\text{O}$ value of the meteoric water from which they precipitated, which is largely controlled by elevation (Drummond et al., 1993a; Dettman and Lohmann, 2000; Garzione et al., 2000a). It is possible to estimate paleoelevation from the oxygen isotope composition of carbonates by using local $\delta^{18}\text{O}_w$ vs. altitude gradients and making assumptions about past climate based on paleoclimate indicators (Drummond et al., 1993a,b; Garzione et al., 2000b; Rowley et al., 2001).

Recent applications of oxygen isotopes to tectonic problems have utilized the proportional decrease of $\delta^{18}\text{O}_w$ with increasing altitude to estimate the paleoelevation of the Tibetan plateau from carbonate rocks deposited on the plateau (Garzione et al., 2000a,b; Rowley et al., 2001; Rowley and Currie, 2002). Several isotopic studies of carbonates have also addressed the Rocky Mountains, where high altitudes, similar to modern, may have been achieved by Late Cretaceous–Eocene time (Drummond et al., 1993a; Norris et al., 1996; Dettman and Lohmann, 2000; Morrill and Koch, 2002). A potential problem in carbonate O isotope paleoaltimetry is diagenetic alteration of the $\delta^{18}\text{O}$ value of carbonate ($\delta^{18}\text{O}_c$). Primary carbonates record the $\delta^{18}\text{O}$ value of meteoric

water from which they precipitated, with some uncertainty due to possible variation in surface temperatures. Diagenesis may take place at higher temperatures or in the presence of fluids with different isotopic compositions, thereby causing a large temperature-dependent fractionation in the $\delta^{18}\text{O}_c$ or producing carbonate with $\delta^{18}\text{O}$ values that reflect waters that moved through the rock at a later time.

Evaluating the diagenetic history of carbonates is particularly important in studies of paleoelevation because diagenesis more commonly causes the $\delta^{18}\text{O}_c$ to become more negative, which would lead to an overestimation of paleoelevation. Most carbonate paleoelevation studies have focused on determining the timing and process by which a region attained its current elevation. Early diagenesis will not modify the $\delta^{18}\text{O}_c$ value if it occurs at similar temperatures to surface temperatures and in equilibrium with the original pore fluids in the carbonate. However, recrystallization at higher temperatures during burial or recrystallization/calcitization in the presence of later fluids moving through the rock can significantly modify the original $\delta^{18}\text{O}_c$, rendering these carbonates useless in studies of paleoelevation (e.g., Morrill and Koch, 2002). Likewise, diagenesis in the presence of later meteoric waters can also lead to a decrease in the $\delta^{18}\text{O}_c$ in regions that have experienced surface uplift since primary carbonate deposition.

As carbonate oxygen isotope paleoaltimetry becomes more widely used, it is important to establish standard practices (thin-section microscopy, stable isotope studies, and carbonate mineralogy) to evaluate the diagenetic history of carbonates to prevent erroneous interpretations of paleoelevation. This paper provides case examples of strategies that can be employed to evaluate the effect of diagenesis on carbonates used in studies of paleoelevation and/or paleoclimatology.

2. Geologic and stratigraphic framework

The three study areas discussed in this paper are located within the Tibetan plateau: the Thakkhola graben in the southern Tibetan plateau, contractional basins in the eastern Tibetan plateau, and Linxia basin within the northeastern margin of the Tibetan plateau (Fig. 1). The Thakkhola graben and basins in eastern

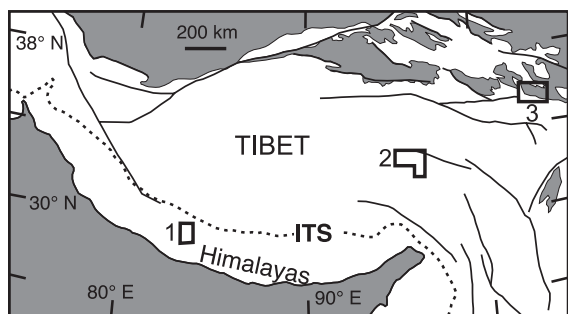


Fig. 1. Regional map showing location of study areas relative to major faults (line traces), Indus–Tsangpo suture (ITS), and Paleogene basins along the periphery of the Tibetan plateau (gray shading). Boxes show the following study areas: (1) Thakkhola graben, (2) Paleogene basins in eastern Tibet, and (3) Linxia basin.

Tibet currently sit at elevations in excess of 3 km, whereas the Linxia basin is situated at an elevation of 1800–2400 m.

2.1. Thakkhola graben

The Thakkhola graben is located north of the high Himalaya and south of the Indus–Tsangpo suture (ITS) within the Tibetan Himalaya. The ITS is the collisional suture between India and Asia. The boundary between the Tibetan Himalaya and the Greater Himalaya, to the south, is marked by a large, low-angle, north dipping, detachment fault, called the South Tibetan Detachment System (Burg and Chen, 1984; Burchfiel et al., 1992). Although the Tibetan Himalaya is geomorphologically continuous with the Tibetan plateau, it is also part of the Himalayan fold-thrust belt and was active mainly during Eocene to Oligocene time (Searle, 1986; Ratschbacher et al., 1994). The oldest age constraints on normal faulting in the Thakkhola graben come from a $^{40}\text{Ar}/^{39}\text{Ar}$ mica age of ~ 14 Ma from a fracture associated with a north-trending fault east of the graben (Coleman and Hodges, 1995). The magnetostratigraphy of the oldest deposits in the graben, the Tetang Formation, best correlates with the geomagnetic polarity time scale between 10.6 and 9.6 Ma (Garzione et al., 2000a). Very negative $\delta^{18}\text{O}$ values for carbonates throughout the history of deposition in the Thakkhola graben have been inferred to indicate elevations similar to modern since the late Miocene onset of deposition in the basin (Garzione et al., 2000a,b).

The Thakkhola graben consists of the Tetang Formation and the <8 Ma Thakkhola Formation (Fort et al., 1981, Garzione et al., 2003) (Fig. 2). The Tetang Formation onlaps remnant topography in folded and thrustured Mesozoic rocks and consists of ~225 m of alluvial fan and fluvial conglomerate, which grades upward into lacustrine deposits (Garzione et al., 2003). An angular unconformity separates the Tetang Formation from the Thakkhola Formation, which is up to ~800 m thick and records

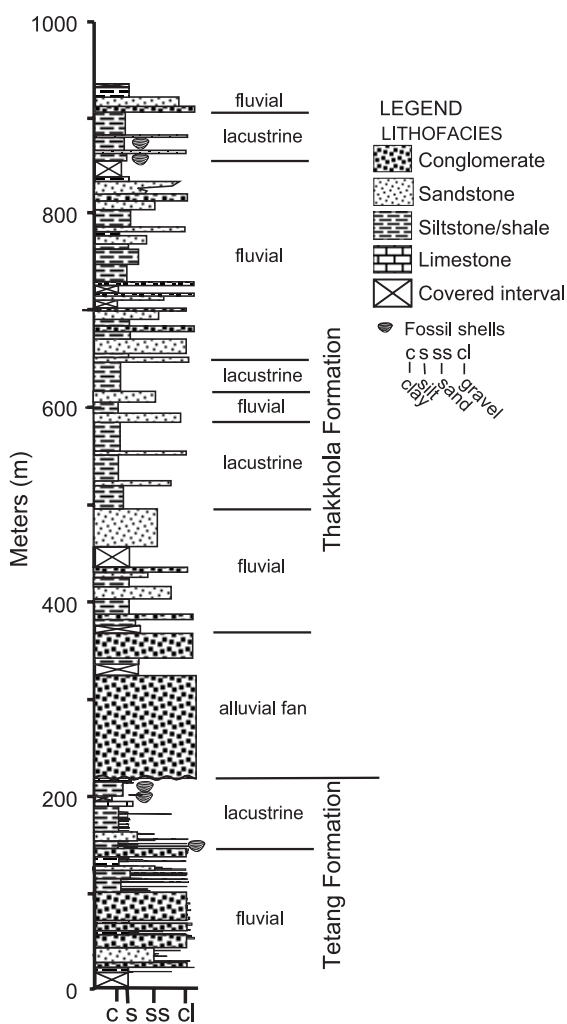


Fig. 2. Composite stratigraphic column of the Thakkhola basin formations showing the location of fossil samples within the Tetang and Chele sections. Refer to Figs. 2, 3, and 4 in Garzione et al. (2003) for more details, including section localities.

a large southward flowing axial river system that experienced intermittent damming as evidenced by widespread lacustrine deposition. Alluvial fan deposits within the Thakkhola Formation are localized along the Dangardzong fault along the western edge of the basin (Garzione et al., 2003). Primary depositional carbonates within the Thakkhola graben include shells and lacustrine micrite within both the Tetang and Thakkhola Formations and pedogenic carbonate within the Thakkhola Formation (Garzione et al., 2003).

2.2. Paleogene basins in eastern Tibet

A series of basins in east-central Tibet (Qinghai BGMR, 1991) (Fig. 3) have been related to Paleogene contractional to transpressional deformation and possible continental subduction during the India–Asia collision (Yin and Harrison, 2000; Wang et al., 2001; Horton et al., 2002). The basins are associated with a thin-skinned, ramp-flat system of northwest-striking thrust faults and related folds developed in predominantly Carboniferous–Triassic carbonates and subordinate siliciclastic rocks (Spurlin et al., 2000). Thrust-related growth strata and narrow basin widths commensurate with thrust spacing indicate that syndepositional shortening controlled basin development (Horton et al., 2002).

The majority of fill in the Nangqian, Niuguoda, Xialaxiu, and Shanglaxiu basins is Paleocene through middle Eocene age based on Paleogene palynomorphs and plant fossils, and igneous rocks that are interbedded with and cross-cut basin fill (Horton et al., 2002). In the Dongba basin, palynomorphs suggest a possible Miocene age (Qinghai BGMR, 1985).

2.2.1. Dongba basin

An over 2-km-thick measured stratigraphic section in the Dongba basin reveals a predominance of

siliciclastic strata, which is arranged into three upward-coarsening stratigraphic packages (labeled a–c in Fig. 3). Facies assemblages include sandstone, conglomerate and limited amounts of mudrock and carbonate attributed to sedimentation in proximal fan-delta, distal fan-delta, and offshore to nearshore lacustrine depositional environments. Thin intervals of lacustrine carbonate strata generally cap the upward-coarsening packages.

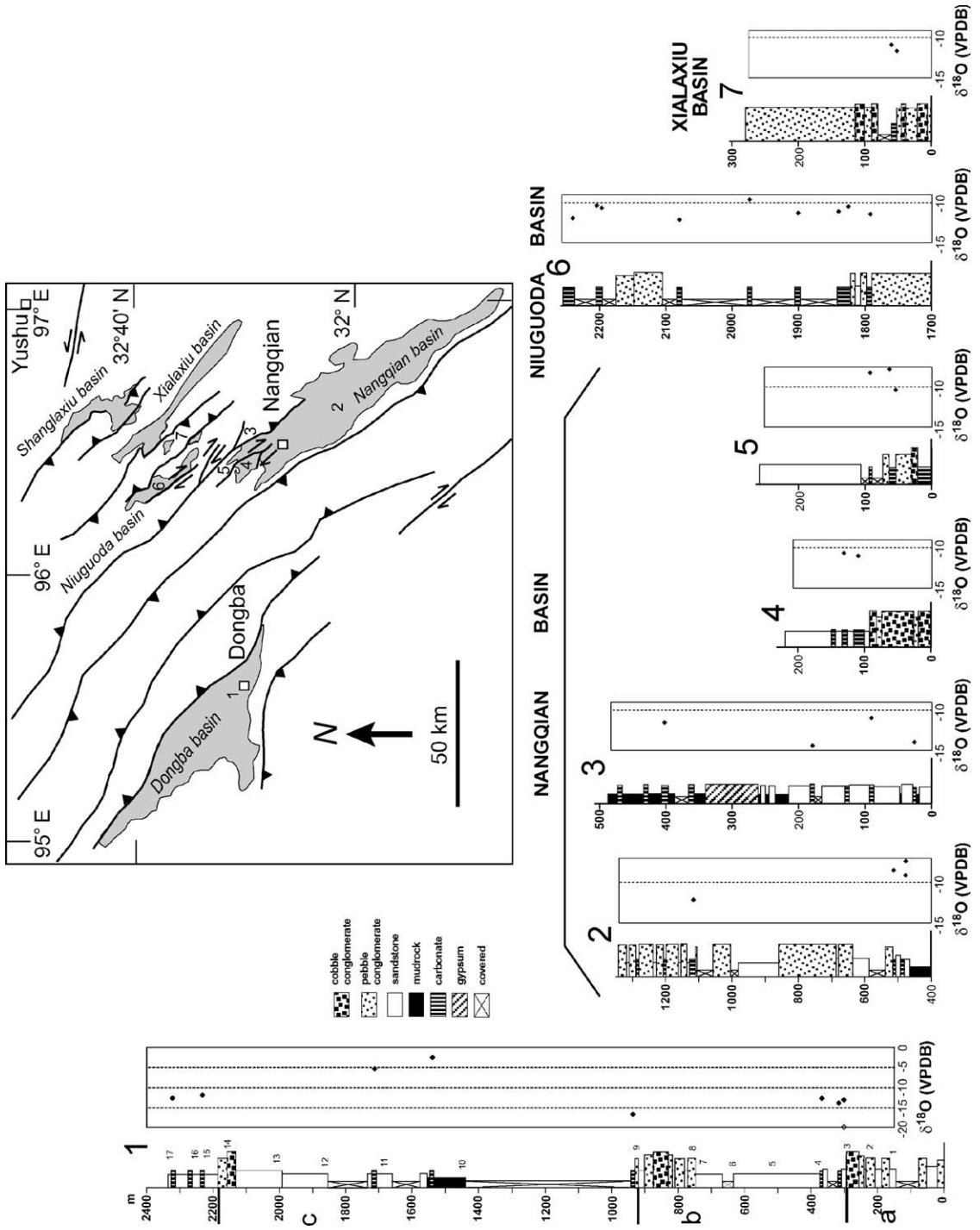
2.2.2. Nangqian, Niuguoda, and Xialaxiu basins

Stratigraphic fill up to 2 km thick characterizes the narrow, elongate Paleocene to Eocene basins between the cities of Nangqian and Yushu (Fig. 3). The upper levels of six measured sections (Fig. 3) are dominated by relatively fine-grained siliciclastic strata (sandstone and mudrock) and subordinate carbonate, interpreted to have been deposited in fan-delta, alluvial-fan, and lacustrine environments (Horton et al., 2002).

2.3. Linxia basin

The Linxia Basin is situated within the northeastern margin of the Tibetan Plateau. Magnetostratigraphy and vertebrate fossil age constraints indicate nearly continuous deposition within Linxia basin between ~29 and 1.8 Ma (Fang et al., 2003; Li et al., 1997). Facies distributions, variations in stratigraphic thickness, and the subsidence history of the Linxia basin suggest that sedimentation occurred in a flexural basin, resulting from loading of the crust adjacent to the deforming NE margin of the Tibetan plateau (Fang et al., 2003). A decrease in subsidence rates associated with thrust faulting in the proximal part of the basin beginning at ~6 Ma and approximately 10° of clockwise rotation of the basin since 8 Ma suggest that the Linxia basin was incorporated into the plateau by late Miocene–early Pliocene time (Fang et al., 2003).

Fig. 3. General tectonic map of study area in east–central Tibetan plateau, modified from Qinghai BGMR (1985, 1991) and measured sections. On map, Paleogene basins (gray shading) are associated with northwest-striking thrust faults (teeth denote upper plate) within predominantly Carboniferous to Triassic strata (no shading). Strike-slip faults (arrows denote sense of slip) postdate basin development. Numerals 1–7 on map refer to measured section locations. Measures sections show stratigraphic and $\delta^{18}\text{O}$ data for section 1 in Dongba basin and sections 2–6 in Nangqian, Niuguoda, and Xialaxiu basins. In measured section 1, three upward-coarsening stratigraphic packages (a–c, separated by horizontal bars) exhibit distal-to-proximal upsection facies variations. Closed symbols denote primary micritic carbonate samples; open symbols denote secondary vein calcite samples. Measured sections 2–6 correspond to sections A, J, L, M, P, and Q, respectively, of Horton et al. (2002).



The Linxia basin is dominated by siliciclastic deposition, with observed thicknesses up to ~1200 m. The stratigraphic section shown in Fig. 4 is a composite of three sections analyzed for stable isotopes in Dettman et al. (2003) and was compiled on the basis of magnetostratigraphic ages defined by Fang et al. (2003). The Maogou section is located in central part of the basin, whereas the Wangjiashan and Dongshanding sections are located more proximal to the margin of the Tibetan Plateau. The oldest deposits in the basin, including the Tala and lower Zhongzhuang Formations, are fluvial (Fig. 4). Widespread lacustrine deposition, recorded in the upper Zhongzhuang through lower Liushu Formations, dominated the basin fill between ~20 and ~7 Ma. The upper part of the basin fill from the middle Liushu Formation through the Dongshan Formation is represented by fluvial and loess deposits. Carbonates within these deposits are rather inconspicuous. Fluvial deposits contain calcite cements and an insignificant percent (~1–3%) detrital carbonate (Dettman et al., 2003). Lacustrine deposits range

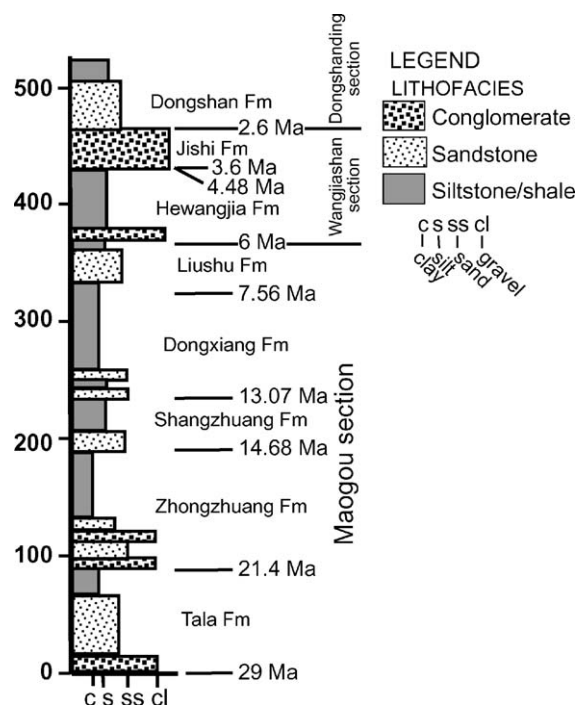


Fig. 4. Composite stratigraphic column of the Linxia basin formations showing general lithology and magnetostratigraphic ages. Refer to Fig. 1 in Fang et al. (2003) for section localities.

from noncalcareous red mudstones to clay-rich beige limestone beds on the order of 1 cm to several 10s of cm thick. These micritic limestone beds can be traced over several kilometers, which suggests that they record times of widespread carbonate formation in the lake. Fluvial calcite cements and lacustrine carbonates in the Linxia basin display a positive shift in oxygen isotope composition in mid-Miocene time, which has been interpreted as representing a change in the source of moisture to the Linxia basin, possibly related to uplift of the Tibetan plateau (Dettman et al., 2003).

3. Methods and materials studied

Diagenetic phases from the Thakkhola graben and eastern Tibet basins and shells from the Thakkhola graben were sampled using a microdrill. The growth bands of shells were milled using a 20- μ m tip in order to separate individual growth increments. The slow growth of these shells did not allow the determination of detailed annual cycles. However, we were able to better resolve the range of isotopic compositions preserved in the shells resulting from seasonal fluctuations in water composition.

The $\delta^{18}\text{O}$ and $\delta^{13}\text{C}$ of micromilled samples were measured using an automated carbonate preparation device (KIEL-III) coupled to a gas-ratio mass spectrometer (Finnigan MAT 252). Samples were heated under vacuum to 200 °C prior to measurement. Powdered samples between 20 and 150 μ g were reacted with dehydrated phosphoric acid under vacuum at 70 °C. Repeated measurements of NBS-19 and NBS-18 were used to calibrate the isotope ratio measurement. Precision is $\pm 0.1\text{‰}$ for $\delta^{18}\text{O}$ and $\pm 0.06\text{‰}$ for $\delta^{13}\text{C}$ (1σ). Larger samples were processed on a manual CO_2 extraction line, and the gas was analyzed on a Finnigan MAT Delta gas-ratio mass spectrometer. Repeated standard measurements yielded precision of $< \pm 0.1\text{‰}$ for $\delta^{18}\text{O}$ and $\pm 0.05\text{‰}$ for $\delta^{13}\text{C}$ (1σ). All carbonate results are reported in VPDB.

4. Results and analyses

Several strategies can be used to evaluate the effects of diagenesis in a terrestrial carbonate record,

including (1) determining the isotopic composition of unambiguous primary carbonate phases, such as aragonite; (2) determining the isotopic composition of diagenetic phases, such as vein calcite or aragonite that have been replaced by calcite; and (3) seeking systematic and high-frequency variation in C and/or O isotopes consistent with other indicators of depositional environment, such as covariance in lake records that reflect changes in the Mg concentration of primary carbonates.

4.1. Aragonite

Aragonitic shell material can be compared to micrite to determine whether the micrite recorded the oxygen isotopic composition of primary carbonate or experienced diagenetic overprinting. Growth bands in shells record seasonal variations in both the temperature and the isotopic composition of the waters from which the shell was precipitated (Dettman et al., 1999). Because lacustrine micrite is highly susceptible to diagenesis and even minor lithification is likely to cause some alteration of micritic carbonate, it is important to assess whether this diagenesis took

place in the presence of original pore waters and at similar temperatures to primary micrite. The seasonal variations in aragonite shell material can be compared to micrite to evaluate whether both carbonates record a similar range in the isotopic composition of paleowater. By this strategy, Morrill and Koch (2002) evaluated the fidelity of the lacustrine micrite record of the Green River Formation originally reported by Norris et al. (1996). Typical values for $\delta^{18}\text{O}_c$ are $\sim -3\text{‰}$, whereas some carbonate horizons as low as -10‰ to -16‰ were interpreted to record seasonal snowmelt input into the lake (Norris et al., 1996). Analysis of both aragonitic and calcitized shell material revealed that primary aragonite shells have values similar to the less negative micrite from the Green River Formation micrites, whereas calcitized shells have more negative values, similar to those that were interpreted as recording snowmelt contributions to the lake (Morrill and Koch, 2002). This calls into question whether the more negative micrites reported by Norris et al. (1996) have also experienced diagenesis that has modified their primary $\delta^{18}\text{O}_c$ values (Morrill and Koch, 2002).

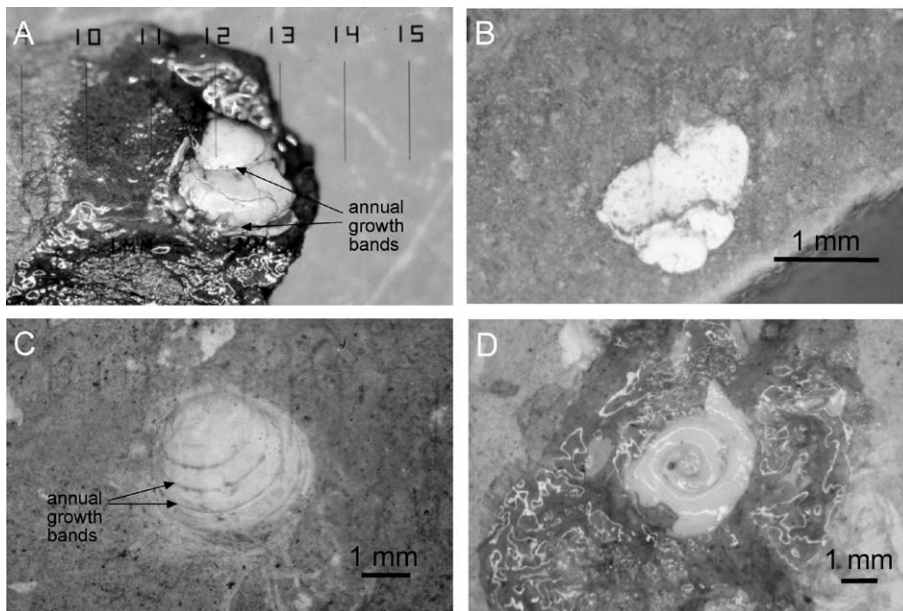


Fig. 5. Fossil bivalves and gastropods from the Tetang and Thakkhola Formations in the Thakkhola graben. (A) *Pisidium* bivalve from 207 m in the Tetang Formation with epoxy coating. Scale shows millimeter increments. (B) Unidentified gastropod from 207 m in the Tetang Formation. (C) *Pisidium* from 647 m in the Thakkhola Formation. (D) *Planorbis* gastropod from 647 m in the Thakkhola Formation with epoxy coating.

Table 1

Oxygen and carbon isotope data from stratigraphic sections sampled in the Thakkhola graben and basins in east-central Tibet

| Sample name | Description | Stratigraphic level | $\delta^{18}\text{O}$ (VPDB) (‰) | $\delta^{13}\text{C}$ (VPDB) (‰) |
|--------------------------------------|-----------------------------------|---------------------|----------------------------------|----------------------------------|
| <i>Thakkhola basin</i> | | | | |
| Tetang Formation | | | | |
| 9TT130a | aragonite gastropod | 145 | −15.2 | −6.1 |
| 9TT130b | aragonite gastropod | 145 | −19.3 | −7.4 |
| 9TT130c | aragonite gastropod | 145 | −23.2 | −9.5 |
| 14TT186a | calcitized pelecypod | 201 | −14.8 | 9.3 |
| 14TT186b | calcitized pelecypod | 201 | −17.4 | 7.9 |
| 14TT186c | calcitized pelecypod | 201 | −17.7 | 7.8 |
| 15TT189 | calcitized gastropod | 204 | −16.2 | 8.3 |
| 17TT192a | calcitized pelecypod ^a | 207 | −11.0 | 9.8 |
| 17TT192b | calcitized pelecypod ^a | 207 | −12.4 | 9.9 |
| 17TT192c | calcitized pelecypod ^a | 207 | −13.3 | 9.5 |
| 17TT192d | calcitized pelecypod ^a | 207 | −12.5 | 9.5 |
| 17TT192e | calcitized pelecypod ^a | 207 | −14.2 | 9.6 |
| 17TT192f | calcitized pelecypod ^a | 207 | −13.5 | 10.2 |
| 17TT192h | calcitized pelecypod ^a | 207 | −13.4 | 9.8 |
| 17TT192i | calcitized pelecypod ^a | 207 | −12.4 | 9.9 |
| 17TT192l | calcitized pelecypod ^a | 207 | −12.5 | 9.5 |
| 17TT192m | calcitized pelecypod ^a | 207 | −13.2 | 9.5 |
| 53TT112 | sparite | 112 | −23.6 | 8.5 |
| | duplicate | | −23.6 | 8.5 |
| 55TT208 | sparite | 208 | −26.0 | 4.7 |
| 54TT211 | sparite | 211 | −22.0 | 7.0 |
| Thakkhola Formation near town of Dhi | | | | |
| 36TH7 | sparite | 7 | −12.6 | 13.1 |
| 36TH7b | sparry gastropod | 7 | −11.9 | 10.2 |
| 36TH7c | sparry gastropod | 7 | −10.7 | 8.0 |
| 36TH7d | sparry gastropod | 7 | −17.9 | 4.4 |
| 43TH257 | micrite | 257 | −22.3 | 0.2 |
| 43TH257a | aragonite pelecypod | 257 | −20.7 | 0.3 |
| 43TH257b | six ostracods | 257 | −20.8 | −1.8 |
| 43TH257c | aragonite pelecypod | 257 | −21.8 | −1.0 |
| 45TH275a | sparry pelecypod | 275 | −17.6 | 4.2 |
| 45TH275b | sparry gastropod | 275 | −20.0 | 10.1 |
| 45TH275c | calcite vein | 275 | −9.2 | 7.4 |
| <i>East-central Tibet basins</i> | | | | |
| Triassic | | | | |
| 00C37 | coarse-grained sparite | | −9.8 | 3.6 |
| 00C39 | fine-grained sparite | | −3.1 | 3.2 |
| 00C39 | calcite vein | | −12.1 | 1.5 |
| 00C41 | coarse-grained sparite | | −6.8 | 3.6 |
| 00C43 | calcite vein | | −11.5 | 2.1 |
| Dongba basin | | | | |
| 00C20 | micrite | 365 | −12.6 | 0.8 |
| 00C21a | calcite vein | 309 | −19.8 | 1.9 |
| 00C21b | micrite | 309 | −12.9 | 1.3 |
| 00C21c | calcite vein | 309 | −19.8 | 2.2 |
| 00C23 | micrite | 317 | −13.8 | 0.6 |
| 00C24 | micrite | 930 | −16.5 | 0.7 |
| 00C25 | micrite | 1526 | −2.5 | −3.6 |
| 00C26 | micrite | 1695 | −5.3 | 0.5 |
| 00C27 | micrite | 2225 | −11.8 | 0.5 |
| 00C28 | micrite | 2300 | −12.6 | −1.9 |

Table 1 (continued)

| Sample name | Description | Stratigraphic level | $\delta^{18}\text{O}$ (VPDB) (‰) | $\delta^{13}\text{C}$ (VPDB) (‰) |
|----------------------------------|--------------------|---------------------|----------------------------------|----------------------------------|
| <i>East-central Tibet basins</i> | | | | |
| Nanqian basin | | | | |
| 00C11 | micrite | 109 | −11.2 | −1.0 |
| 00C13 | calcite vein | 130 | −10.5 | 0.7 |
| 00C14 | micrite | 53 | −10.2 | −0.2 |
| 00C15 | micrite | 64 | −7.7 | −1.1 |
| 00C16 | micrite | 91 | −8.2 | −1.0 |
| 00C17 | micrite | 402 | −11.5 | 5.0 |
| 00C19 | micrite | 90 | −11.0 | −4.2 |
| 00C29 | micrite | 483 | −8.4 | −1.8 |
| 00C29a | calcite vein | 483 | −7.3 | −1.6 |
| 00C29b | sparite | 483 | −9.0 | −1.5 |
| 00C32 | micrite | 511 | −8.4 | −0.7 |
| 00C33 | micrite | 1113 | −12.1 | −2.8 |
| Niubuoda basin | | | | |
| 00C1 | micrite | 1790 | −11.4 | 3.2 |
| 00C2 | micrite | 1823 | −10.4 | 3.0 |
| 00C3 | micrite | 1836 | −11.1 | 4.4 |
| 00C4 | micrite | 1900 | −11.3 | 4.0 |
| 00C5 | micrite | 1972 | −9.6 | 3.4 |
| 00C6 | calcite vein | 2080 | −12.1 | 0.0 |
| 00C7 | calcite vein | 2195 | −10.7 | 5.2 |
| 00C8 | micrite | 2202 | −10.3 | 5.0 |
| 00C9 | micrite | 2240 | −11.9 | 2.0 |
| Xialaxiu basin | | | | |
| 00C45 | micrite with veins | 52 | −11.6 | 3.0 |
| 00C46 | micrite with veins | 53 | −10.8 | 2.9 |

Thakkhola data not included are micrites, paleosol carbonate, and aragonitic shells from the Thakkhola Formation previously published in Garzione et al. (2000a).

$\delta^{13}\text{C}$ errors = $\pm 0.05\text{‰}$ and $\delta^{18}\text{O}$ errors = ± 0.1 based on standard measurements and duplicate sample runs.

Vienna PeeDee belemnite (VPDB).

^a Denotes shell growth bands that were micromilled.

4.1.1. Thakkhola graben

Lacustrine micrite and paleosol carbonate deposited in the Thakkhola graben in the southern Tibetan plateau have been interpreted to indicate similar to modern elevations since the earliest deposition in the basin (late Miocene) based on very negative $\delta^{18}\text{O}_\text{c}$ values of -13‰ to -23‰ (Garzione et al., 2000a,b). Marginal lacustrine deposits of the Tetang Formation contain *Pisidium* bivalves and unidentified gastropods (Fig. 5A and B). The overlying Thakkhola Formation contains abundant paleosol carbonates and occasional palustrine carbonates, associated with fluvial deposits. Palustrine intervals 0.5–2 m thick sometimes contain *Pisidium* and *Planorbis* gastropods (Fig. 5C and D).

By comparing aragonite shell material with lacustrine and paleosol micrite in the Tetang and Thakkhola Formations, it can be established whether micrites

record paleosurface water compositions within the Thakkhola graben. Most of the shell material collected from the Tetang Formation was calcified. Because of the small size of the shells (1 and 2.5 mm in their longest dimension) and the sparseness of shell material, we determined shell composition using a Feigl stain test (Feigl, 1958; Friedman, 1959). Bivalves and gastropods sampled in the upper part of the Tetang Formation (between 201 and 207 m) (Fig. 2) were calcitic and were powdery and white. The only aragonitic shell material from the Tetang Formation was collected at 145 m. These fragments of a crushed gastropod shell were deposited in a fluvial channel during a lowstand in lake level. The shells retained a pink color and nacreous luster. Three individual fragments, each less than 1 mm, yielded extremely variable $\delta^{18}\text{O}_\text{c}$ values of -15.2‰ to -23.2‰ (Table 1, Fig.

6A). The calcitized pelecypod shells, however, displayed a smaller range of $\delta^{18}\text{O}_c$ values and were more positive than the aragonitic gastropod shells. The ranges of $\delta^{18}\text{O}$ values in each of two microsampled shells were -14.8‰ to -17.4‰ and -11‰ to -14.2‰ (Fig. 6A).

In the Thakkhola Formation, the southernmost section near the town of Chele yielded the greatest number of carbonate samples. One bed at 647 m from the bottom of the Thakkhola Formation contained abundant *Planorbis* and *Pisidium* 3–4 mm long. Two bivalves were micromilled to determine the range in $\delta^{18}\text{O}$ values recorded in the shells, however individual growth bands were too thin to determine high resolution seasonal variations in $\delta^{18}\text{O}$ values. Analysis of two micromilled shells and one whole *Pisidium* shell shows a range of -16.8‰ to -21.1‰ in $\delta^{18}\text{O}_c$ values (Table 1, Fig. 6B).

In order to compare the $\delta^{18}\text{O}_w$ values required to produce the observed aragonite and calcite $\delta^{18}\text{O}$ values, we calculated $\delta^{18}\text{O}_w$ values using the temperature-dependent fractionation equations for oxygen isotopes during calcite precipitation (Kim and O'Neil, 1997) and aragonite precipitation (Grossman and Ku, 1986, as modified in Dettman et al., 1999). Lacustrine carbonate tends to become supersaturated during the summer when evaporation rates are highest and carbonates have the lowest solubility, which leads to whitening events during a discrete time period when the lake water is warm (e.g., Duston et al., 1986, Effler et al., 1987). Because micrite forms during a similar time period every year, temperature variations often do not have a large effect on the $\delta^{18}\text{O}$ of lacustrine carbonate (McKenzie, 1985; McKenzie and Hollander, 1993; Drummond et al., 1995; Hodell et al., 1998). We therefore used the average temperature for the warmest month (July) of $14\text{ }^\circ\text{C}$ for the town of Lo Manthang (elevation 3750 m) in the northern part of the basin as an approximation of the temperature of calcite and aragonite formation (Nepal Department of Hydrology and Meteorology, 1996). Likewise, paleosol carbonates precipitate during the summer growing season as plants remove water from the soil by evapotranspiration (Cerling and Wang, 1996). Although this temperature estimate is based on modern temperatures, it is probably reasonable within $\pm 5\text{ }^\circ\text{C}$ given that middle to late Miocene equatorial sea surface temperatures were similar to today (Savin

et al., 1985) and the paleoelevation of the Thakkhola graben was also similar to modern elevation in this region (Garziona et al., 2000a,b; Rowley et al., 2001). Note that the $\delta^{18}\text{O}$ value of water calculated from the carbonate isotope composition is not highly sensitive to the temperature selected; an uncertainty of $\pm 4.5\text{ }^\circ\text{C}$ leads to an uncertainty of only 1‰ in the calculated $\delta^{18}\text{O}$ of the water (Kim and O'Neil, 1997; Dettman et al., 1999).

In both the Tetang and Thakkhola Formations, the $\delta^{18}\text{O}_w$ values required to produce the observed $\delta^{18}\text{O}$ values of aragonitic shells, lacustrine micrites, and pedogenic carbonate nodules are very similar. The gastropod deposited in a fluvial channel in the Tetang Formation indicates a wide range of $\delta^{18}\text{O}_w$ compositions of -16.5‰ to -24.5‰ and compares well with the range of $\delta^{18}\text{O}_w$ values between -17.1‰ and -23.3‰ calculated from the $\delta^{18}\text{O}$ values of lacustrine micrite. The wider range observed in the shell fragments may be associated with larger seasonal fluctuations in the $\delta^{18}\text{O}_w$ value of river water as compared to lake water fluctuations which are buffered by the larger volume of water in the lake. The interpretation that this gastropod was associated with fluvial water is further supported by the carbon isotope data, which indicates $\delta^{13}\text{C}$ values more than 5‰ more negative than all other lacustrine micrite values. The $\delta^{13}\text{C}$ value of dissolved inorganic carbon (DIC) in lake systems is relatively more enriched than fluvial water that supplies the lake because of the preferential uptake of ^{12}C by photosynthetic organisms in the lake (McKenzie, 1985) and the preferential outgassing of ^{12}C -rich CO_2 from the surface of the lake (Talbot, 1990).

In the Thakkhola Formation, calculated $\delta^{18}\text{O}_w$ values for aragonite ranged between -18.1‰ and -22.4‰ and for micrite and paleosol carbonates ranged between -13‰ and -22.3‰ . The three micrite samples from slackwater pond deposits (less than 50 cm thick) within fluvial successions indicate $\delta^{18}\text{O}_w$ values of -19.4‰ to -19.7‰ , which fall within the range of $\delta^{18}\text{O}_w$ values estimated from the shells. However, five of the 20 paleosol carbonate samples yielded more positive $\delta^{18}\text{O}_w$ estimates than the shells. One possible explanation for the more positive waters derived from paleosols relates to the source of water. The ponds were probably fed by overflow from the laterally adjacent fluvial system,

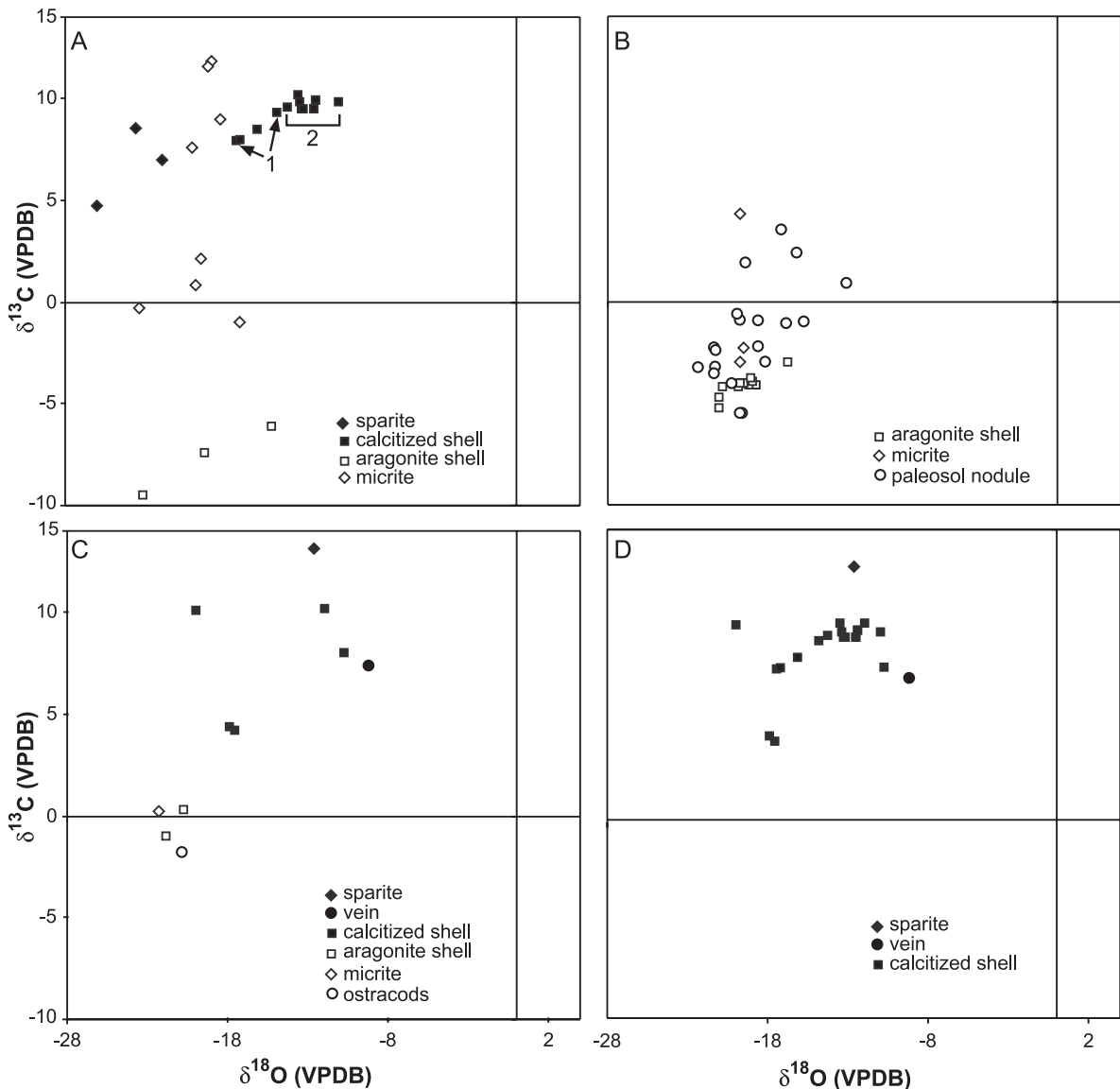


Fig. 6. O and C data from Thakkhola graben carbonates. Refer to Fig. 2 in Garzione et al. (2003) for section localities. (A) Data from the Tetang Formation near Tetang village. 1 and 2 show micromilled samples from two bivalves sampled at 207 m. (B) Data from the Thakkhola Formation near Chele village. (C) Data from the Thakkhola Formation near Dhi village. (D) Diagenetic carbonates from the Dhi village section and calcitized shells of the Tetang village section showing the overlap in O and C isotopic compositions between some diagenetic carbonates of both the Tetang and Thakkhola Formations.

which sourced water from a range of higher elevations. Soils, on the other hand, are likely to receive most of their moisture from rainfall that occurs locally within the basin. Therefore, the more negative values in the slackwater pond micrites and shells may reflect higher elevation rainfall and snowmelt sourced by the river

system which fed these ponds, whereas paleosol carbonates may record local lower elevation rainfall within the basin.

The conclusion that can be drawn from this comparison of aragonite and lacustrine micrite data is that the general consistency between the calculated

$\delta^{18}\text{O}_w$ values of these carbonates suggests that micrites record the $\delta^{18}\text{O}_c$ values of primary carbonate. Although these micrites have experienced early diagenesis, this diagenesis occurred in equilibrium with primary pore fluids in the micrites and at similar temperatures to water temperatures in the lake. However, calcitized shells of the Tetang Formation record $\delta^{18}\text{O}_c$ values up to $\sim 4\%$ more positive than aragonitic shell material, which suggests that calcitization occurred in the presence of later fluids. This diagenetic event will be further discussed in the following section on diagenetic phases in the Thakkhola graben.

4.2. Diagenetic phases

In some cases, analysis of various diagenetic phases can provide insight into whether the $\delta^{18}\text{O}$ values of primary carbonates have been modified. If

the $\delta^{18}\text{O}_c$ values of diagenetic phases differ from micrites in a way that is consistent with the history of diagenesis, then it can be assumed that the micrite records the $\delta^{18}\text{O}$ values of the paleometeoric water from which it precipitated.

4.2.1. Thakkhola graben

Carbonates of the Thakkhola graben have a complicated history characterized by several different phases of diagenesis. In thin section, micrites from the central part of the basin have primary pore spaces that are usually filled with very fine-grained blocky calcite, suggesting a phase of early diagenesis (Fig. 7A). In the eastern part of the basin, lacustrine carbonates of the Tetang Formation have extensive dissolution cavities filled with coarse-grained sparry calcite and have undergone significant recrystallization. Thin sections show that 30–65% of the sample has been recrystallized (Fig. 7B). Along the eastern

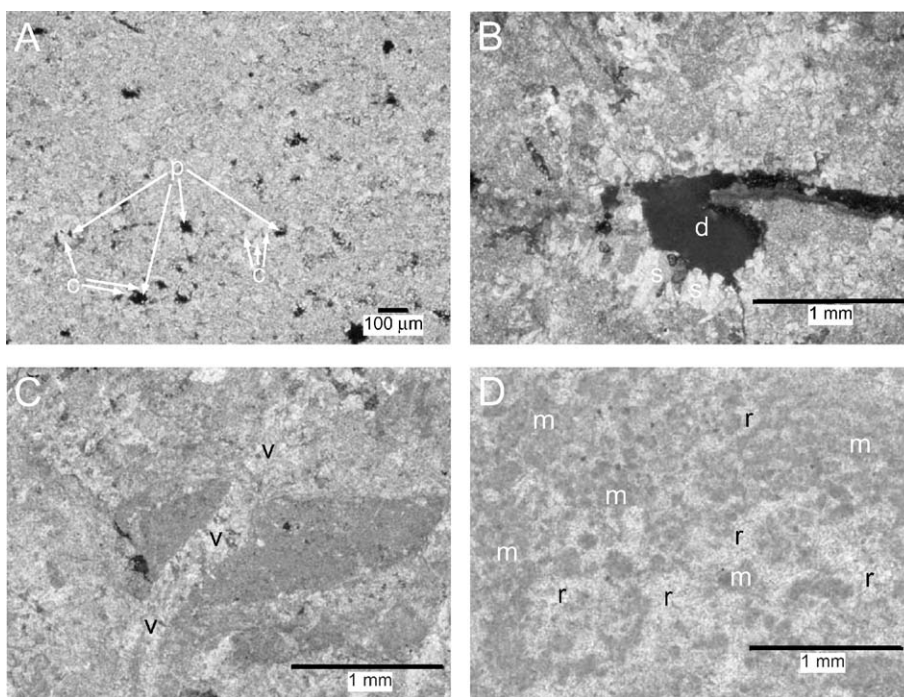


Fig. 7. Photomicrographs from the Tetang and Thakkhola Formations in southern Tibet and carbonates from east-central Tibet. All images were taken under cross-polarized light and converted to grayscale. (A) Carbonate from the Tetang Formation in the central part of the Thakkhola graben, showing several pore spaces (p) indicated by arrows and coarser blocky calcite crystals (c) that fill these pores spaces. (B) Examples of dissolution cavity (d) within Tetang Formation carbonates in the eastern part of the basin and infilling by growth of coarse calcite (s). (C) Calcite vein (v) within Thakkhola Formation carbonate in the northeastern part of the Thakkhola graben. (D) Typical limestone from east-central Tibet showing the extent of fine-grained recrystallization (r) of primary micrite (m).

side of the basin in the Thakkhola Formation, micrite and shells have undergone extensive, coarse-grained calcitization, associated with calcite veins (Fig. 7C).

Stable carbon isotopes of lacustrine carbonates from the Tetang Formation have high $\delta^{13}\text{C}$ [Vienna PeeDee belemnite (VPDB)] values of -1 to 12‰ , which gives insight into the lacustrine paleoenvironment. Primary lake carbonates record the carbon isotopic composition of DIC in the upper water column of the lake at the time of carbonate precipitation. The isotopic composition of DIC is a function of inflow composition, exchange with atmospheric CO_2 at the lake's surface, reduction of organic matter in the lake, and water residence times (McKenzie, 1985; Talbot and Kelts, 1990). High primary productivity in a lake can increase $\delta^{13}\text{C}$ values to slightly positive values, but values over 4‰ are rare. $\delta^{13}\text{C}$ values vs. $\delta^{18}\text{O}$ values for lacustrine carbonates of the Tetang Formation yield a vertical array, with constant $\delta^{18}\text{O}$ values and highly variable $\delta^{13}\text{C}$ values (Fig. 6A). Talbot and Kelts (1990) documented a similar vertical array from organic-rich lake deposits in Ghana, with lower $\delta^{13}\text{C}$ values observed in primary carbonate and higher $\delta^{13}\text{C}$ values in diagenetically altered carbonates. Values of $\delta^{13}\text{C}$ as high as 26‰ were attributed to methanogenic processes that fractionated C during the breakdown of organic material after burial (Talbot and Kelts, 1990). Based on the extremely positive $\delta^{13}\text{C}$ values in early diagenetic carbonates of the Tetang Formation, we infer that bottom water conditions were dysaerobic in these lakes, leading to the breakdown of organic matter by bacterial methanogenesis. This early diagenesis affected the C isotope composition of carbonates, but had a minimal effect on O isotopes because it occurred in the presence of the original pore fluids in the sediment (Talbot and Kelts, 1990) as evidenced by the similarity between the oxygen isotope composition of aragonite shell material and micrite (Fig. 6A).

Tetang Formation sparites from the eastern part of the basin have slightly more negative $\delta^{18}\text{O}_\text{c}$ values than micrites from the central part on the basin. Three sparite samples show $\delta^{18}\text{O}_\text{c}$ values between -22‰ and -26‰ , which is up to 2.6‰ more negative than the most negative micrite value. These more negative values suggest that the sparite formed at a higher temperature than micrite, perhaps after burial of the

Tetang Formation. A shift of $\sim -3\text{‰}$ between micrite and sparite requires a temperature of sparite formation of $\sim 15^\circ\text{C}$ higher than micrite formation. Assuming a typical geothermal gradient for young continental crust of $\sim 30^\circ\text{C}/\text{km}$, this temperature difference would be consistent with burial on the order of 500 m. This amount of burial is reasonable given the thickness of up to 800 m for the overlying Thakkhola Formation.

Burial diagenesis cannot explain the more positive $\delta^{18}\text{O}_\text{c}$ values observed in the calcitized shells of the Tetang Formation (Table 1, Fig. 6A). These altered shells have similar values to diagenetic phases in the Thakkhola Formation sampled near Dhi. Coarse sparite, vein calcite and calcitized shells in the Dhi section have $\delta^{18}\text{O}_\text{c}$ values and $\delta^{13}\text{C}$ values of -20‰ to -9.2‰ and 4.2‰ to 13.1‰ , respectively (Table 1, Fig. 6C). These values are elevated in both $\delta^{18}\text{O}_\text{c}$ values and $\delta^{13}\text{C}$ values with respect to a micritic bed (257 m) sampled in the same section containing unaltered gastropods (Fig. 6C). The similarity between the calcitized shells in the Tetang Formation and diagenetic phases in the Dhi section in the Thakkhola Formation suggests a similar origin for the diagenetic fluids in both of these formations. In a study of the chemistry of Himalayan river and stream water in the Kali Gandaki drainage and several other drainage basins across the Nepal Himalaya, Galy and France-Lanord (1999) found extremely high $\delta^{13}\text{C}$ values of dissolved inorganic carbon ($\delta^{13}\text{C}_{\text{DIC}}$) in tributaries and the main stem of the Kali Gandaki within the Thakkhola graben, with values as high as 3.9‰ . South of the Thakkhola graben, the Kali Gandaki and its tributaries have $\delta^{13}\text{C}_{\text{DIC}}$ values that range between -10‰ and 0‰ . Springs sampled in the Thakkhola graben at the contact between sedimentary fill and basement yielded $\delta^{13}\text{C}_{\text{DIC}}$ that were highly enriched in ^{13}C , with values in excess of 10‰ . These extremely positive values cannot be explained by CO_2 sourced from the atmosphere, plants, and/or the dissolution of carbonates, but instead require a source of metamorphic CO_2 (Galy and France-Lanord, 1999). At temperatures of $300\text{--}400^\circ\text{C}$, metamorphic decarbonization produces dry CO_2 enriched by $2\text{--}6\text{‰}$ with respect to the source rock (Shieh and Taylor, 1969; Friedman and O'Neil, 1977). The dissolution of CO_2 in groundwater produces HCO_3^- with $\delta^{13}\text{C}$ values that are $6\text{--}10\text{‰}$ higher than the gas (Mook et al., 1974). If a metamorphic source for CO_2 is responsible

for the higher $\delta^{13}\text{C}$ values in diagenetic carbonates of the Tetang and Thakkhola Formation, then the $\delta^{18}\text{O}$ values of the waters that source this CO_2 would also have to be more positive to explain the higher $\delta^{18}\text{O}_\text{c}$ values in these samples. Thermal waters can experience relatively more equilibration with silicate and carbonate rocks, which drives the $\delta^{18}\text{O}_\text{w}$ to more positive values (Craig, 1963). Craig (1966) showed that the magnitude of this positive shift increases with increasing temperature. This can be explained by the fact that the fractionation factor decreases with increasing temperature, leading to $\delta^{18}\text{O}_\text{w}$ values that approach rock $\delta^{18}\text{O}$ values. Therefore, it is likely that diagenetic carbonates in the Thakkhola graben, which record both elevated $\delta^{18}\text{O}_\text{c}$ values and $\delta^{13}\text{C}$ values (Fig. 6D), were formed during the interaction of thermal waters.

4.2.2. Paleogene basins in east–central Tibet

We sampled micritic carbonates in shortening-related, lacustrine-dominated basins at 4–5 km elevation in the east–central Tibetan plateau for interpretation of paleoelevation and paleoclimate. Isotopic data for secondary calcite veins within Paleogene lacustrine carbonates and for recrystallized Carboniferous–Triassic marine carbonate, the local bedrock, were collected to evaluate the possible complicating effects of diagenesis.

The degree of diagenetic alteration was assessed through thin-section microscopy. Micritic carbonates display extensive microcrystalline recrystallization, making it difficult to microsample unaltered primary micrite (Fig. 7D).

Paleogene lacustrine micrites in east–central Tibet have $\delta^{18}\text{O}$ values of predominantly -9% to -12% (PDB). The full range of values is -9% to -12% for the Nangqian, Niuguoda, and Xialaxiu basins and -2% to -16% for the Dongba basin (Figs. 3 and 8). Secondary calcite veins within Paleogene carbonate beds have $\delta^{18}\text{O}$ values of -20% for the Dongba basin, -10.5 to -12% for the Niuguoda and Xialaxiu basins, and -7% to -10.5% for the Nangqian basin.

Diagenetic effects related to vein calcite formation can explain some of the differences between stable isotopic values (both $\delta^{18}\text{O}$ and $\delta^{13}\text{C}$) of the host micrite vs. the calcite veins. However, it is difficult to distinguish the degree of isotopic change that has taken place within the micrites associated with

diagenesis. For example, vein calcites in the Dongba basin (Fig. 8A) have $\delta^{18}\text{O}$ values as low as -20 , which are more than 3% more negative than the most negative micrite value, whereas the $\delta^{13}\text{C}$ values of the vein calcites are more positive than micrites. This difference in C isotopes suggests an additional source of DIC other than the micrite. The lower $\delta^{18}\text{O}$ values in the vein carbonates likely resulted from either calcite formation at higher temperatures or from waters with more negative $\delta^{18}\text{O}$ values. The micrite data display a linear trend, which shows increasing enrichment in ^{13}C with increasing depletion in ^{18}O , with vein calcites at one end of the spread in data (Fig. 8A). We interpret this spread to indicate that varying degrees of diagenesis in the micrites may have caused enrichment in ^{13}C and depletion in ^{18}O , thereby obscuring the original isotopic composition of the micrites.

In the Nangqian basin, calcite veins fall within the range of $\delta^{18}\text{O}$ and $\delta^{13}\text{C}$ values observed in micrites (Fig. 8B). It is possible to interpret these data in two ways. Either vein calcite precipitated from meteoric water of the same isotopic composition as micrites or the micrites have been significantly modified by the same diagenetic fluids that formed the veins. Similar difficulties exist for Niuguoda and Xialaxiu basins, in that values for vein calcites plot at both ends of the array of micrite data (Fig. 8C), leaving open the possibility that the micrites were modified during the diagenesis that led to vein formation. Recrystallized Carboniferous through Triassic marine carbonates on the northern margins of the Nangqian basin provide evidence of the degree of diagenesis that the Paleogene lacustrine micrites may have experienced, because we can assume that their original oxygen isotopic composition of marine carbonate was close to 0% . All of these marine carbonates have been extensively recrystallized, although some preserve microcrystalline grain sizes and others exhibit coarse-grained recrystallization. The $\delta^{18}\text{O}$ values of -3% to -10% observed in these bedrock samples are substantially more negative than typical marine carbonate (Fig. 8D). This decrease in $\delta^{18}\text{O}$ values could have been caused by diagenetic alteration during the interaction of more negative meteoric water of different composition, such as modern meteoric water. Alternatively, recrystallization under higher temperature conditions may account for the

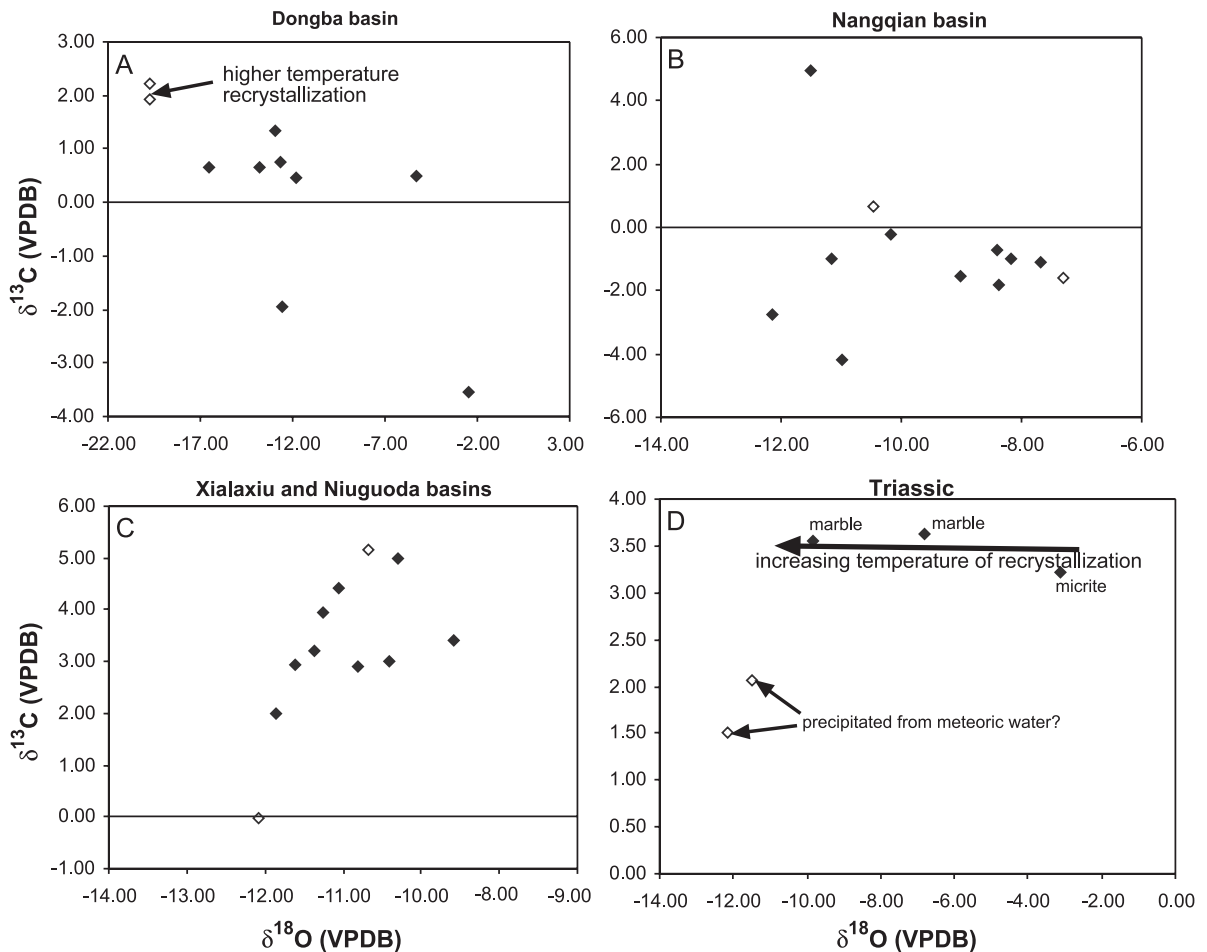


Fig. 8. Plots of $\delta^{18}\text{O}$ vs. $\delta^{13}\text{C}$ for (A) Dongba basin, (B) Nangqian basin, (C) Niuguoda and Xialaxiu basins, and (D) Carboniferous–Triassic carbonate. Closed symbols denote carbonate rock composition; open symbols denote vein calcite composition.

lower $\delta^{18}\text{O}$ values. Vein calcite in these rocks have slightly more negative $\delta^{18}\text{O}_c$ values of -11% and -12% and fall within the range of values observed in veins in Nangxian, Niuguoda, and Xialaxiu basins. The similarity in vein isotopic composition among the different basins suggests that all of these carbonates experienced diagenesis under similar temperature conditions and/or by interaction with meteoric water of similar isotopic composition.

Lacustrine micrite and vein calcite from Nangxian, Niuguoda, and Xialaxiu basins can be compared to modern meteoric water to determine the possible source of waters that formed these carbonates. Two sets of river water samples were collected in eastern Tibet. A larger collection of 36 samples from the

northeastern Tibetan plateau, from 2 to 3.3 km elevation, exhibit $\delta^{18}\text{O}$ values of predominantly -8% to -11% SMOW (Fig. 9, Table 2). Samples define an approximate northeast to southwest transect from lower to higher elevation. There is a clear decrease in $\delta^{18}\text{O}$ values from 2 to 2.8 km. The most negative $\delta^{18}\text{O}$ values occur at ~ 2.8 km. Above 2.8 km, however, there are several samples with distinctively less negative $\delta^{18}\text{O}$ values (Fig. 9). As discussed by Araguás-Araguás et al. (1998), this seemingly odd relationship may result from evaporation of raindrops below the cloud base in this semiarid region or evaporation from surface water. A smaller collection of three samples of river waters in east–central Tibet, in the Nangqian–Yushu region ($32\text{--}33^\circ\text{N}$, $96\text{--}97^\circ\text{E}$),

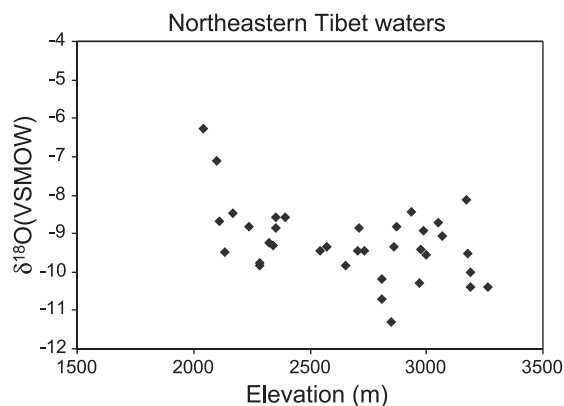


Fig. 9. Plot of altitude vs. $\delta^{18}\text{O}$ for river waters ($n=36$) sampled in northeastern Tibet, southwest of Linxia basin.

yielded $\delta^{18}\text{O}$ values from -10.5% to -12.5% . In central Tibet at $33\text{--}35^\circ\text{N}$, $91\text{--}92^\circ\text{E}$, $\delta^{18}\text{O}$ values for precipitation (rain-gauge) and river waters are -9% to -12% (Tian et al., 2001), quite similar to the modern values reported here for eastern Tibet. Assuming a temperature of $15\text{--}16^\circ\text{C}$ for calcite precipitation, consistent with observed water temperatures during the summer months in modern lakes of the Tibetan plateau (Lister et al., 1991; Fontes et al., 1996; Wei and Gasse, 1999), the $\delta^{18}\text{O}_w$ values calculated for Paleogene lacustrine micrites are similar to modern meteoric waters. These similarities can be interpreted in two ways. Either lower Paleogene lacustrine micrites in eastern Tibet were deposited in a similar paleogeographic and paleoclimatic setting as today or these micrites have been diagenetically altered to reflect the isotopic composition of modern meteoric water.

4.3. Chemical variability in lake records

Lake waters commonly display covariance between O and C isotopes where increases in $\delta^{18}\text{O}_w$ are reflected by increases in the $\delta^{13}\text{C}$ of DIC (Talbot, 1990; Drummond et al., 1995). Covariance between C and O isotopic ratios in primary lacustrine carbonates has been attributed to closed basin conditions (Talbot, 1990) and/or seasonal or longer time scale climate variations in open lake systems (Drummond et al., 1995). Covariance can also result from partial diagenesis, where the covariant trend is a mixing line between the unaltered and diagenetic carbonate. Thus,

simply demonstrating a covariant trend does not say much about the presence or absence of alteration. However, when the pattern of variability is strongly tied to other chemical changes expected in lacustrine carbonate, and when this variation is preserved on small spatial or temporal scales, an argument can be made for the preservation of primary carbonate (e.g., Drummond et al., 1993b).

4.3.1. Linxia basin

Lacustrine carbonates deposited in the Linxia basin between ~ 20 and 7 Ma have the appearance of primary lacustrine precipitates based on sedimentary textures and stratigraphy. They are poorly lithified, and there is no evidence of secondary cement or diagenetic phases. The carbonate rich intervals are discreet layers, $1\text{--}40$ cm thick, that follow bedding planes within the fine grain siliciclastic sediments that make up the lake deposits. In a few of these beds, poorly preserved molds of gastropods and ostracodes have been observed. These features suggest that these carbonates had their origin in "whiting events," times when the lake water was supersaturated with respect to carbonate, and micrite was deposited throughout the lake basin. However, the observation that fossils have been dissolved indicates that some diagenesis has occurred, and therefore diagenesis must be considered in the interpretation of carbonate isotopic compositions.

More than 50 of these layers exist in the 200-m thick lacustrine interval in the Maogou section. These lake deposits, from 20 to 7 Ma show relatively high frequency alternation between a relatively stable more negative $\delta^{18}\text{O}$ value and a more variable more positive end member (Fig. 10A). This variation also shows C and O isotope covariance (Fig. 10B), which has been interpreted as the variation between open and closed lake conditions (Dettman et al., 2003). During open basin conditions, water flows through the lake system, little or no evaporation takes place, and the $\delta^{18}\text{O}$ of the lake water is not changed by evaporation. Therefore, the $\delta^{18}\text{O}$ of lake water in an open lake should approach values of inflowing water derived primarily from rainfall in the basin. Increases in $\delta^{18}\text{O}_c$ of 2% to 6% are most likely associated with basin closure and an increase in the degree of evaporation, which increases the $\delta^{18}\text{O}$ of lake water. The parallel movement of $\delta^{13}\text{C}$ to more positive values could be the result of nutrient concentration and increased

Table 2
Oxygen isotopic data and elevation information for sampled tributaries in NE Tibet

| Sample name | Tributary/village name | Sampling elevation (m) | Sampling location | $\delta^{18}\text{O}$ (VSMOW) (‰) |
|-------------|------------------------|------------------------|---------------------------|-----------------------------------|
| 01cw37 | Wangjiashan village | 2041 | N35°37.104', E102°04.463' | -6.3 |
| 01cw35 | unnamed | 2097 | N35°27.872', E103°01.156' | -7.1 |
| 01cw34 | unnamed | 2112 | N35°27.007', E102°00.020' | -8.7 |
| 01cw33 | unnamed | 2133 | N35°26.651', E102°59.104' | -9.5 |
| 01cw32 | unnamed | 2169 | N35°25.460', E102°57.197' | -8.5 |
| 01cw1 | Xianggao village | 2237 | N35°24.428', E102°55.940' | -8.8 |
| 01cw3 | Qingshui River | 2285 | N35°21.875', E102°52.729' | -9.8 |
| | duplicate | 2285 | N35°21.875', E102°52.729' | -9.8 |
| 01cw29 | unnamed | 2325 | N35°21.959', E102°51.200' | -9.2 |
| 01cw28 | unnamed | 2343 | N35°21.626', E102°50.270' | -9.3 |
| 01cw2 | unnamed | 2352 | N35°22.771', E102°53.446' | -8.8 |
| | duplicate | 2352 | N35°22.771', E102°53.446' | -8.6 |
| 01cw27 | unnamed | 2395 | N35°19.238', E102°47.014' | -8.6 |
| 01cw26 | unnamed | 2541 | N35°14.175', E102°49.637' | -9.4 |
| 01cw9 | unnamed | 2572 | N35°11.500', E102°49.536' | -9.3 |
| 01cw10 | unnamed | 2654 | N35°11.159', E102°49.288' | -9.8 |
| 01cw11 | Luolang River | 2704 | N35°05.482', E102°54.027' | -9.5 |
| 01cw25 | unnamed | 2710 | N34°38.867', E103°32.678' | -8.8 |
| 01cw24 | Yangsha village | 2732 | N34°45.955', E103°37.764' | -9.4 |
| 01cw4 | Jiangma village | 2810 | N35°12.462', E102°40.371' | -10.2 |
| 01cw7 | unnamed | 2848 | N35°11.987', E102°37.904' | -11.3 |
| 01cw6 | Shanggashi village | 2863 | N35°11.670', E102°37.564' | -9.4 |
| 01cw19 | Azitan village | 2874 | N34°43.171', E103°10.403' | -8.8 |
| 01cw21 | unnamed | 2938 | N34°43.529', E103°22.789' | -8.4 |
| 01cw12 | Zhaolu village | 2970 | N34°56.061', E102°54.947' | -10.3 |
| 01cw18 | unnamed | 2973 | N34°46.173', E103°13.003' | -9.4 |
| 01cw22 | unnamed | 2986 | N34°44.592', E103°33.231' | -8.93 |
| 01cw20 | unnamed | 2999 | N34°44.118', E103°23.753' | -9.6 |
| 01cw23 | unnamed | 3052 | N34°44.828', E103°33.666' | -8.7 |
| 01cw5 | unnamed | 3070 | N35°09.345', E102°25.626' | -9.1 |
| 01cw16 | unnamed | 3172 | N34°50.891', E103°05.801' | -8.1 |
| 01cw17 | unnamed | 3177 | N34°50.325', E103°09.692' | -9.5 |
| 01cw13 | Hezuo River | 3191 | N34°52.268', E102°58.392' | -10.4 |
| 01cw14 | unnamed | 3191 | N34°52.268', E102°58.392' | -10 |
| 01cw15 | unnamed | 3263 | N34°52.071', E103°02.855' | -10.4 |

Data for each location appear in order from lowest to highest sampling elevation.

Elevations and locations were determined using a Garmin Model 45 GPS unit.

Vienna standard mean ocean water (VSMOW).

productivity in a closed lake, or outgassing of CO_2 during closed basin conditions (Talbot, 1990).

The mineralogy of these carbonates also alternates between two end members, low-magnesian calcite and dolomite, with a strong relationship to the $\delta^{18}\text{O}$ of the carbonate (Fig. 10C). More negative $\delta^{18}\text{O}$ values are associated with low-Mg calcite (<4 mol% Mg). Carbonates with more positive $\delta^{18}\text{O}$ values are dolomite and intermediate values are some mixture of the two. Dolomite precipitation in lake sediments is strongly associated with closed,

saline lakes (Last, 1990). Low-Mg calcite is a common mineral in open, low salinity, marl lakes (Duston et al., 1986; Effler et al., 1987). This reinforces the idea that the more negative $\delta^{18}\text{O}$ value is associated with open lake conditions and more positive $\delta^{18}\text{O}$ values represent closed and evaporative lake conditions. In support of this interpretation, similar trends between $\delta^{18}\text{O}$ values and mineralogy have been observed in the Early Cretaceous Peterson limestone, deposited in the Cordilleran foreland in Wyoming (Drummond et

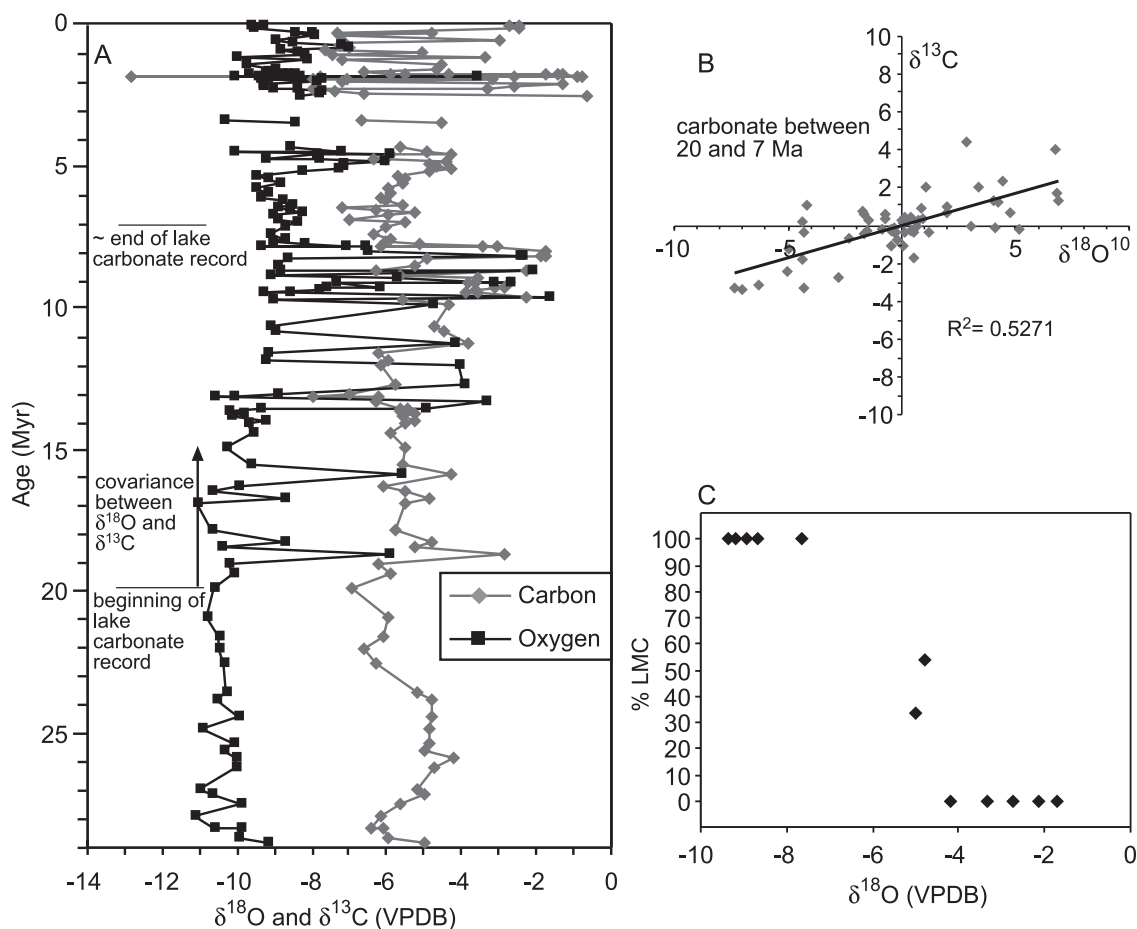


Fig. 10. (A) Plot of $\delta^{18}\text{O}$ and $\delta^{13}\text{C}$ in Linxia basin carbonates. Note that increases in $\delta^{18}\text{O}$ are associated with increases in $\delta^{13}\text{C}$ during the interval of lacustrine deposition between ~20 and 7 Ma. (B) Isotopic composition of lacustrine carbonates deposited in the Linxia basin between 20 and 7 Ma. Note the covariant trend between $\delta^{18}\text{O}$ and $\delta^{13}\text{C}$. (C) Increase in the % low-Mg calcite (LMC) associated with a decrease in $\delta^{18}\text{O}$ in lacustrine carbonates in the Linxia basin suggests that dolomite was deposited during times of greater evaporation and closed-basin conditions.

al., 1993b, 1996). Both textural and systematic compositional variation in the Peterson limestone suggest that dolomite and calcite are a cogenetic mineral assemblage (Drummond et al., 1993b). Within meter scales beds in the Peterson limestone, lower Mg/Ca ratios and more negative $\delta^{18}\text{O}$ values are associated with deposition of a greater proportion of fine-grained siliciclastic sediment, which has been used to infer that these variations are largely driven by climate change (Drummond et al., 1996).

Although lacustrine carbonates in the Linxia basin seem to have originated as precipitates from lake water, the question of diagenetic alteration of

these carbonates remains a possibility. Could dolomite be the diagenetic phase and the covariance of mineralogy, oxygen and carbon isotopes be due to variable dolomitization? Although we cannot absolutely rule out this possibility it seems unlikely because of the high variability in the system. If diagenesis were the cause of the mineralogical and isotopic changes, it would likely affect all of the carbonates in this section. However, there are no trends from top to bottom and throughout the section there are frequent changes between the two end members (of C and O isotopic composition and mineralogy) over stratigraphic thicknesses at the

submeter level. The high frequency of these shifts supports the view that this is a record of primary lacustrine carbonates.

5. Discussion and conclusions

Oxygen isotope paleoaltimetry is based on the observation that topography has a significant effect on the degree of rain-out (condensation out of a vapor mass). As elevation increases, the decrease in temperature and relative humidity drive rain-out, causing the $\delta^{18}\text{O}$ and $\delta^2\text{H}$ values of meteoric water to become more negative with increasing elevation (Siegenthaler and Oeschger, 1980; Rowley et al., 2001; Gonfiantini et al., 2001). The variation in $\delta^{18}\text{O}_w$ with altitude can be modeled and compared to authigenic carbonates to estimate the elevation of carbonate deposition (Garzione et al., 2000b; Rowley et al., 2001). The $\delta^{18}\text{O}$ values of pedogenic carbonates may reflect the local elevation of rainfall in the basin, whereas $\delta^{18}\text{O}$ values of lacustrine carbonates may record the complex integration of elevations in catchments basins of rivers that fed the lake. Determining the diagenetic history of micritic carbonates is a critical step in oxygen isotope paleoaltimetry studies. Diagenesis commonly takes place (1) at higher elevations than original carbonate deposition and (2) under conditions that produce more negative $\delta^{18}\text{O}_c$. Either an increase in the temperature of calcite formation or precipitation of calcite from later higher elevation meteoric water can cause erroneously high estimates of paleoelevation. Likewise, an increase in $\delta^{18}\text{O}_c$ values and underestimate of actual paleoelevation can result from diagenetic carbonates that precipitated from thermal waters, which approach the value of carbonate or silicate rocks through which the waters have circulated.

The most robust means of determining the fidelity of a carbonate record is to measure carbonate phases that are known to have escaped alteration, such as aragonitic shell material, for comparison to the micrite record. In the Thakkhola graben, unaltered shells from both the older Tetang Formation and younger Thakkhola Formation produce similar calculated $\delta^{18}\text{O}_w$ values for paleometeoric water, which indicates that the micrite record is reliable.

When shells are not available, the analysis of different diagenetic phases for O and C isotopic compositions can also shed light on the effects of diagenesis on micrites. Anomalously positive $\delta^{13}\text{C}$ values with little change in $\delta^{18}\text{O}$ values in lacustrine micrites of the Tetang Formation may have resulted from early diagenesis by methanogenic processes. Sparites in the Tetang Formation have more negative $\delta^{18}\text{O}$ values than micrites by several per mil, which suggests these rocks experienced recrystallization under higher temperatures, possibly during burial. Yet another phase of diagenesis is recorded by the calcitization of shells in both the Tetang and Thakkhola Formations and calcite veins in the Thakkhola Formation. These carbonates have elevated $\delta^{13}\text{C}$ and $\delta^{18}\text{O}$ values, which can be explained by diagenesis during the interaction of thermal waters. In the Thakkhola graben, early diagenesis has had a minimal effect on the $\delta^{18}\text{O}$ values of micrites, whereas later diagenesis by thermal waters and during burial has produced significantly modified isotopic compositions in diagenetic carbonates.

For Paleogene basins in eastern Tibet, the similarity in the isotopic composition of micrites and vein carbonates makes the interpretation of these data equivocal. Vein carbonates plot as end members or within C and O trends in the micrite data. This may indicate that both micrites and vein carbonates precipitated from meteoric water of similar isotopic composition or that micrite isotopic compositions have been modified to reflect vein carbonate compositions. Very negative $\delta^{18}\text{O}$ values reported from Eocene deposits in the Lunpola basin have been interpreted to indicate very high elevation in central Tibet during Eocene time (Rowley and Currie, 2002). However, it is conceivable that these deposits have experienced diagenesis considering their age, tectonic setting, and the thickness of basin fill. Both oxygen and carbon isotopic compositions from diagenetic phases within the Lunpola basin and other basins in the Tibetan plateau would provide insight on the history of diagenesis, providing a more complete evaluation of the elevation estimates from central Tibet.

The source of covariance in lacustrine deposits of Linxia basin can be examined through the mineralogy of lake carbonates. Diagenesis can lead to increases in both $\delta^{18}\text{O}$ and $\delta^{13}\text{C}$, which may appear to indicate covariance related to lacustrine processes. However,

other geochemical signatures can help determine whether the covariance reflects the composition of primary carbonate. Under more evaporative conditions, lakes tend to precipitate more high-Mg calcite and dolomite as opposed to low-Mg calcite (Last, 1990). Therefore, examining the carbonate mineralogy can elucidate the causes of covariance in the lake record. Lacustrine carbonates in Linxia basin are dominated by low-Mg calcite, and dolomite, with high-Mg calcite present in trace amounts. Comparing the percentage of low-Mg calcite to the oxygen isotopic composition of the lake demonstrates that carbonate intervals with higher $\delta^{18}\text{O}$ values are associated with a greater percentage of dolomite and high-Mg calcite (Fig. 10c). Correspondence between these two indicators and variation on a scale consistent with lake processes suggest that this variance is a function of water residence time in the lake rather than diagenesis.

Acknowledgements

The authors thank D. Hodkinson, T.P. Ojha, B.N. Upreti, Fang Xiaomin, Dr. Song Chunhui, Fan Majie and Zhou Jiangyu for field assistance. This research was supported by NSF grants EAR9510033 and EAR9905887 (to Dettman) and EAR0106677 (to Horton). We are grateful to C. Drummond, A. Longinelli, and Finn Surlyk for thoughtful reviews, which helped us improve this paper.

References

- Araguás-Araguás, L., Froehlich, K., Rozanski, K., 1998. Stable isotope composition of precipitation over southeast Asia. *J. Geophys. Res.* 103, 28721–28742.
- Burchfiel, B.C., Chen, Z., Hodges, K.V., Liu, Y., Royden, L.H., Deng, C., Xu, J., 1992. The south Tibetan detachment system, Himalayan orogen: extension contemporaneous with and parallel to shortening in a collisional mountain belt. *GSA Spec. Pap.*, 269.
- Burg, J.P., Chen, G.M., 1984. Tectonics and structural zonation of southern Tibet, China. *Nature* 311, 219–223.
- Cerling, T.E., Wang, Y., 1996. Stable carbon and oxygen isotopes in soil CO_2 and soil carbonates: theory, practice, and application to some prairie soils of upper Midwestern North America. In: Boutton, T.W., Yamasaki, S. (Eds.), *Mass Spectrometry of Soils*. Marcel Dekker, New York, NY, pp. 113–131.
- Coleman, M., Hodges, K., 1995. Evidence for Tibetan plateau uplift before 14 Myr ago from a new minimum age for east–west extension. *Nature* 374, 49–52.
- Craig, H., 1963. The isotopic geochemistry of water and carbon in geothermal areas. In: Tongiorgi, E. (Ed.), *Nuclear Geology on Geothermal Areas*, Spoleto, 1963. Consiglio Nazionale delle Ricerche, Laboratorio di Geologia Nucleare, Pisa, pp. 17–53.
- Craig, H., 1966. Isotopic composition and origin of the Red Sea and Salton Sea geothermal brines. *Science* 154, 1544–1548.
- Department of Hydrology and Meteorology, Precipitation Records of Nepal, 1974–1994, 1996. His Majesty's Government of Nepal, Ministry of Water Resources, Department of Hydrology and Meteorology, Kathmandu, Nepal.
- Dettman, D.L., Lohmann, K.C., 2000. Oxygen isotope evidence for high altitude snow in the Laramide Rocky Mountains of North America during the late Cretaceous and Paleogene. *Geology* 28, 243–246.
- Dettman, D.L., Reische, A.K., Lohmann, K.C., 1999. Controls on the stable isotope composition of seasonal growth bands in aragonite fresh-water bivalves (Unionidae). *Geochim. Cosmochim. Acta* 63, 1049–1057.
- Dettman, D.L., Fang, X., Garziona, C.N., Li, J., 2003. Uplift-driven climate change at 12 Ma: a long $\delta^{18}\text{O}$ record from the NE margin of the Tibetan plateau. *Earth Planet. Sci. Lett.* 6764, 1–11.
- Drummond, C.N., Wilkinson, B.H., Lohmann, K.C., Smith, G.R., 1993a. Effect of regional topography and hydrology on the lacustrine isotopic record of Miocene paleoclimate in the Rocky Mountains. *Palaeogeogr. Palaeoclimatol. Palaeoecol.* 101, 67–79.
- Drummond, C.N., Wilkinson, B.H., Lohmann, K.C., 1993b. Rock-dominate diagenesis of lacustrine magnesian calcite micrite. *Carbonates Evaporites* 8, 214–223.
- Drummond, C.N., Patterson, W.P., Walker, J.C.G., 1995. Climatic forcing of carbon–oxygen isotopic covariance in temperate-region marl lakes. *Geology* 23, 1031–1034.
- Drummond, C.N., Wilkinson, B.H., Lohmann, K.C., 1996. Climatic control of fluvial-lacustrine cyclicity in the Cretaceous Cordilleran Foreland Basin, western United States. *Sedimentology* 43, 677–689.
- Duston, N.M., Owen, R.M., Wilkinson, B.H., 1986. Water chemistry and sedimentological observations in Littlefield Lake, Michigan: implications for lacustrine marl deposition. *Environ. Geol. Water Sci.* 8, 229–236.
- Effler, S.W., Greer, H., Perkins, M.G., Field, S.D., Mills, E., 1987. Calcium carbonate precipitation and transparency in Lakes: a case study. *J. Environ. Eng.* 113, 124–133.
- Fang, X., Garziona, C.N., Van der Voo, R., Li, Jijun, Fan, Majie, 2003. Flexural subsidence by 29 Ma on the NE Edge of Tibet: magnetostratigraphy of Linxia Basin, China. *Earth Planet. Sci. Lett.* 210, 545–560.
- Feigl, F., 1958. *Spot Tests in Inorganic Analysis*, 5th edition. Elsevier, Amsterdam.
- Fontes, J.C., Gasse, F., Gilbert, E., 1996. Holocene environmental changes in Lake Bangong basin (Western Tibet): Part 1. Chronology and stable isotopes of carbonates of a Holocene lacustrine core. *Palaeogeogr. Palaeoclimatol. Palaeoecol.* 120, 25–47.

- Fort, M., Bassoulet, J.P., Colchen, M., Freydet, P., 1981. Sedimentological and structural evolution of the Thakkhola–Mustang graben (Nepal Himalaya) during Late Neogene and Pleistocene. Neogene/Quaternary Boundary Field Conference, India, 1979. Geological Survey of India, Calcutta, India. pp. 25–35. Proceeding.
- Friedman, G.M., 1959. Identification of carbonate minerals by staining methods. *J. Sediment. Petrol.* 29, 87–97.
- Friedman, I., O'Neil, J.R., 1977. Compilation of stable isotope fractionation factors of geochemical interest. U.S.G.S. Professional Paper 440-KK.
- Galy, A., France-Lanord, C., 1999. Weathering processes in the Ganges–Brahmaputra basin and the riverine alkalinity budget. *Chem. Geol.* 159, 31–60.
- Garzione, C.N., Dettman, D.L., Quade, J., DeCelles, P.G., Butler, R.F., 2000a. High times on the Tibetan Plateau: paleoelevation of the Thakkhola graben, Nepal. *Geology* 28, 339–342.
- Garzione, C.N., Quade, J., DeCelles, P.G., English, N.B., 2000b. Predicting paleoelevation of Tibet and the Himalaya from $\delta^{18}\text{O}$ vs. altitude gradients of meteoric water across the Nepal Himalaya. *Earth Planet. Sci. Lett.* 183, 215–229.
- Garzione, C.N., DeCelles, P.G., Hodkinson, D.G., Ojha, T.P., Upreti, B.N., 2003. East–west extension and Miocene environmental change in the southern Tibetan plateau, Thakkhola graben, central Nepal. *Geol. Soc. Amer. Bull.* 115, 3–20.
- Gonfiantini, R., Roche, M.A., Olivry, J.C., Fontes, J.C., Zuppi, G.M., 2001. The altitude effect on the isotopic composition of tropical rains. *Chem. Geol.* 181, 147–167.
- Grossman, E.L., Ku, T.L., 1986. Oxygen and carbon isotope fractionation in biogenic aragonite: temperature effects. *Chem. Geol.* 59, 59–74.
- Hodell, D.A., Schelske, C.L., Fahnenstiel, G.L., Roberts, L.L., 1998. Biologically induced calcite and its isotopic composition in Lake Ontario. *Limnol. Oceanogr.* 43, 187–190.
- Horton, B.K., Yin, A., Spurlin, M.S., Zhou, J., Wang, J., 2002. Paleocene–Eocene syncontractional sedimentation in narrow, lacustrine-dominated basins of east–central Tibet. *Geol. Soc. Amer. Bull.* 114, 771–786.
- Kim, S.T., O'Neil, J.R., 1997. Equilibrium and nonequilibrium oxygen isotope effects in synthetic carbonates. *Geochim. Cosmochim. Acta* 61, 3461–3475.
- Last, W.M., 1990. Lacustrine dolomite: an overview of modern, Holocene, and Pleistocene occurrences. *Earth Sci. Rev.* 27, 221–263.
- Li, J., Fang, X., Van der Voo, R., Zhu, J., MacNiocaill, C., Cao, J., Zhong, W., Chen, H., Wang, J., Wang, J., Zhang, Y., 1997. Late Cenozoic magnetostratigraphy (11–0 Ma) of the Dongshanding and Wangjiashan sections in Longzhong Basin, western China. *Geol. Mijnb.* 76, 121–134.
- Lister, G.S., Kelts, K., Zao, C.K., Yu, J.Q., Niesses, F., 1991. Lake Qinghai, China: closed basin lake levels and the oxygen isotope record for ostracoda since the latest Pleistocene. *Palaeogeogr. Palaeoclimatol. Palaeoecol.* 84, 141–162.
- McKenzie, J.A., 1985. Carbon isotopes and productivity in the lacustrine and marine environment. In: Stumm, W. (Ed.), *Chemical Processes in Lakes*. Wiley, New York, NY, pp. 99–118.
- McKenzie, J.A., Hollander, D.J., 1993. Oxygen isotope record in recent sediments from Lake Greiffen, Switzerland (1750–1986): application of continental isotopic indicator for evaluation of changes in climate and atmospheric circulation patterns. In: Swart, P., Lohmann, K.C., McKenzie, J.A., Savin, S. (Eds.), *Climate Change in Continental Isotopic Records*. American Geophysical Union Monograph, vol. 78, pp. 101–111.
- Mook, W.G., Bommerson, J.C., Staverman, W.H., 1974. Carbon isotope fractionation between dissolved bicarbonate and gaseous carbon dioxide. *Earth Planet. Sci. Lett.* 22, 169–176.
- Morrill, C., Koch, P.L., 2002. Elevation or alteration? Evaluation of isotopic constraints on paleoaltitudes surrounding the Eocene Green River Basin. *Geology* 30, 151–154.
- Norris, R.D., Jones, L.S., Corfield, R.M., Cartlidge, J.E., 1996. Skiing in the Eocene Uinta Mountains? Isotopic evidence in the Green River Formation for snowmelt and large mountains. *Geology* 24, 403–406.
- Poage, M.A., Chamberlain, C.P., 2001. Empirical relationships between elevation and the stable isotope composition of precipitation and surface waters: considerations for studies of paleoelevation change. *Am. J. Sci.* 301, 1–15.
- Qinghai BGMR (Qinghai Bureau of Geology and Mineral Resources), 1985. Geologic map of the Dongba region (1:200,000 scale): unpublished.
- Qinghai BGMR (Qinghai Bureau of Geology and Mineral Resources), 1991. Regional Geology of Qinghai Province. Geological Publishing House, Beijing.
- Ratschbacher, L., Frisch, W., Liu, G., Chen, C., 1994. Distributed deformation in southern and western Tibet during and after the India–Asia collision. *J. Geophys. Res.* 99, 19917–19945.
- Rowley, D.B., Currie, B.S., 2002. Cenozoic paleoaltimetry and paleohypsometry of the Himalayas and Tibet plateau. *Abstr. Programs-Geol. Soc. Am.* 34, 472.
- Rowley, D.B., Pierrehumbert, R.T., Currie, B.S., 2001. A new approach to stable isotope-based paleoaltimetry: implications for paleoaltimetry and paleohypsometry of the High Himalaya since the Late Miocene. *Earth Planet. Sci. Lett.* 188, 253–268.
- Savin, S.M., Hodell, D., Kennett, J.P., Murphy, M., Keller, G., Killingley, J., Vincent, E., 1985. The evolution of Miocene surface and near-surface marine temperatures: oxygen isotopic evidence. *Geol. Soc. Am. Mem.* 163, 49–73.
- Searle, M.P., 1986. Structural evolution and sequence of thrusting in the high Himalaya, Tibetan Tethys and Indus suture zones of Zaskar and Ladakh, western Himalaya. *J. Struct. Geol.* 8, 923–936.
- Shieh, Y.N., Taylor, H.P., 1969. Oxygen and carbon isotope studies of contact metamorphism of carbonate rocks. *J. Petrol.* 10, 307–331.
- Siegenthaler, U., Oeschger, H., 1980. Correlation of ^{18}O in precipitation with temperature and altitude. *Nature* 285, 314–317.
- Spurlin, M., Yin, A., Harrison, T.M., Horton, B.K., Zhou, J., Wang, J., 2000. Two phases of Cenozoic deformation in east–central Tibet: thrusting followed by right-slip faulting. *Eos Trans., Am. Geophys. Union* 81, 1092.

- Talbot, M.R., 1990. A review of the paleohydrological interpretation of carbon and oxygen isotopic ratios in primary lacustrine carbonates. *Chem. Geol.* 80, 261–279.
- Talbot, M.R., Kelts, K., 1990. Paleolimnological signatures from carbon and oxygen isotopic ratios in carbonates from organic carbon-rich lacustrine sediments. *Lacustrine Basin Exploration—Case Studies and Modern Analogs*. AAPG Memoir, vol. 50, pp. 99–112.
- Tian, L., Masson-Delmotte, V., Stievenard, M., Yao, T., Jouzel, J., 2001. Tibetan plateau summer monsoon northward extent revealed by measurements of water stable isotopes. *J. Geophys. Res.* 106, 28081–28088.
- Wang, J.H., Yin, A., Harrison, T.M., Grove, M., Zhang, Y.Q., Xie, G.H., 2001. A tectonic model for Cenozoic igneous activities in the eastern Indo-Asian collision zone. *Earth Planet. Sci. Lett.* 188, 123–133.
- Wei, K., Gasse, F., 1999. Oxygen isotopes in lacustrine carbonates of West China revisited; implications for post glacial changes in summer monsoon circulation. *Quat. Sci. Rev.* 18, 1315–1334.
- Yin, A., Harrison, T.M., 2000. Geologic evolution of the Himalayan–Tibetan orogen. *Annu. Rev. Earth Planet. Sci.* 28, 211–280.